SIMULATION OF THE COMPLETE RESIN INFUSION PROCESS

Quentin Govignon, Simon Bickerton, Piaras A Kelly

FPCM-9 (2008)
The 9th International Conference on Flow Processes in Composite Materials
Montréal (Québec), Canada
8 ~ 10 July 2008

SIMULATION OF THE COMPLETE RESIN INFUSION PROCESS

Q. Govignon [1], S. Bickerton [1, 3], P. A. Kelly [2]

Centre for Advanced Composite Materials,
[1] *Department of Mechanical Engineering,*
[2] *Department of Engineering Science,*
The University of Auckland, Private Bag 92019, Auckland 1020, New Zealand
[3] *Corresponding author's Email: s.bickerton@auckland.ac.nz*

SUMMARY: Resin Infusion (a.k.a. VARTM) is one of the Liquid Composite Moulding processes, for which liquid resin is drawn into dry fibre reinforcement. Resin Infusion is a closed mould process in which half of the mould is formed by a flexible vacuum bag. Significant cavity thickness changes occur during processing, due to the flexibility of the vacuum bag and the complex stress balance within the laminate. While the magnitude of thickness change is often small, the influence is significant on reinforcement fibre volume fraction. Dynamic changes in permeability during mould filling and post-filling have the potential to significantly affect the process. To simulate this behaviour, it is important to accurately model the compaction and relaxation of reinforcement in the dry and wet state. A series of tests have been completed to determine the compaction behaviour of an isotropic glass fibre mat. From these tests several non-linear elastic compaction models have been determined, and applied within a new Resin Infusion simulation. The process simulation, which addresses the pre-filling, filling and post-filling stages, is compared to an experiment employing a full field cavity thickness measurement apparatus, as well as measurement of resin pressure at three discrete points within the laminate.

KEYWORDS: Resin Infusion (RI), simulation, monitoring

INTRODUCTION

Resin Infusion (RI) is part of the Liquid composite Moulding (LCM) process family. The term LCM describes the closed mould processes in which a liquid polymeric resin is impregnated through a fibrous reinforcement. Common LCM processes are Resin Transfer Moulding (RTM), Injection/Compression Moulding (I/CM), RTM-Light and Resin Infusion (RI). LCM processes provide good control over harmful volatiles generated by thermoset resins, making them compliant with tougher new environmental standards put in place internationally. The final fibre volume fraction (V_f) achieved can be higher and more consistent than with traditional open mould techniques. LCM processes also have potential for automation, greatly reducing labour costs.

As opposed to the RTM and I/CM processes, RI uses a single sided mould, the cavity being sealed by a vacuum bag. The compaction of the fibrous reinforcement is governed by the pressure difference between the cavity and the atmospheric pressure. Fig. 1 describes the different components required for application of RI, and the different process stages. Initially, layers of fibrous reinforcement are laid on the mould to form the preform. Distribution media can be laid over the preform to enhance resin flow if the reinforcement has low in-plane permeability. Once inlet and vent tubes are in place, the mould is closed using a vacuum bag sealed with sealant tape. With the cavity sealed, the inlet is clamped and vacuum is applied to the vents, this stage being referred to here as "pre-filling". At the end of pre-filling, the inlet is opened and the resin penetrates the preform. During the "filling stage", pressure inside the cavity varies in position and time. Once the resin front reaches the end of the preform, the inlet is usually clamped. The "post-filling" stage involves removal of excess resin, and allows resin pressure to equilibrate within the cavity. Once the resin is fully cured, the vacuum is released and the part is lifted off the mould and separated from the consumables.

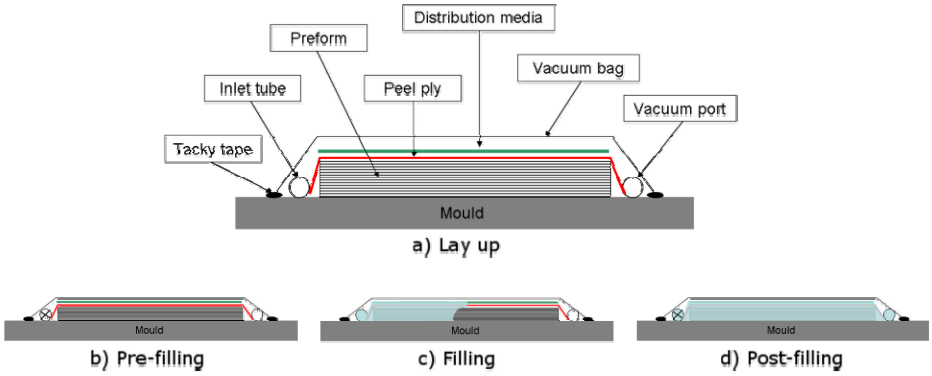

Fig. 1 Four stages of the resin infusion process.

This paper describes a 1D simulation of the RI process including the pre-filling, filling and post-filling stages. To validate the simulation, a detailed RI experiment is presented. In this experiment the fluid is injected along one edge of a rectangular preform, and vacuum is applied along the opposite edge. If race-tracking is correctly eliminated along the edges of the preform and no distribution media is used, the process can then be assumed as purely 1D.

THEORY

Resin Flow

Resin flow through a fibrous reinforcement is usually described using Darcy's law;

$$q_x = -\frac{K}{\mu}\frac{dP}{dx}, \qquad (1)$$

where q_x represents the volume-averaged velocity, K is the permeability of the preform, μ is the fluid viscosity and P is the local fluid pressure. The conservation of solid and fluid mass imposes:

$$-\frac{\partial(q_x h)}{\partial x} = \frac{\partial h}{\partial t}, \tag{2}$$

where h is the local laminate thickness. Combining Eqns. 1 and 2 gives;

$$\frac{\partial}{\partial x}\left(\frac{K}{\mu} h \frac{\partial P}{\partial x}\right) = \frac{\partial h}{\partial t}. \tag{3}$$

Using a non-mixed method with conservative elements [1], q_x at the flow front can be approximated as follows. Using linear finite elements, the first derivative of the pressure is constant over an element. Using a Taylor series about the centre of the element one finds that:

$$q_x = -\frac{K}{\mu}\frac{\partial P}{\partial x} + (x - x_c)\frac{\partial q_x}{\partial x}. \tag{4}$$

As thickness and hence permeability vary spatially, the velocity gradient and local velocity are:

$$\frac{\partial q_x}{\partial x} = \frac{\partial}{\partial x}\left(-\frac{K}{\mu}\frac{\partial P}{\partial x}\right) = -\frac{1}{\mu}\left(\frac{\partial K}{\partial x}\frac{\partial P}{\partial x} + K\frac{\partial^2 P}{\partial x^2}\right), \tag{5}$$

$$q_x = -\frac{K}{\mu}\frac{\partial p}{\partial x} + \left(\frac{x - x_c}{h}\right)\left(\frac{K}{\mu}\frac{\partial P}{\partial x} - \frac{\partial h}{\partial t}\right). \tag{6}$$

Reinforcement Behaviour

The modified Carman-Kozeny equation is often used to relate permeability and V_f:

$$K = C\frac{\left(1 - V_f\right)^{n+1}}{{V_f}^n}, \tag{7}$$

where C and n are parameters determined from experiment. The permeability of the 450 g/m^2 Chopped Strand Mat (CSM) used this study, was measured at various V_f during steady state flow experiments. C and n were found to be 8.7x10^{-11} m^2 and 2.55 respectively.

V_f is dependant on the compaction stress applied to the preform. It has been demonstrated that fibrous reinforcements have complex compaction behaviour, exhibiting viscoelasticity and permanent deformation [2-5]. These materials also display a change of rigidity between the dry and saturated state. During RI, fibre compaction is governed by the difference between atmospheric pressure and pressure inside the cavity, which can be stated as:

$$\sigma_f = P_{atm} - P, \tag{8}$$

where σ_f is the local fibre compaction stress, and P_{atm} is the atmospheric pressure.

During RI, reinforcement follows three compaction phases. During pre-filling, the vacuum is applied and the reinforcement is subjected to a ‘dry compaction’. During the filling stage, the

saturated part of the reinforcement is subjected to a ‘wet unloading’ as the local fluid pressure increases. Then during post-filling, the fluid pressure decreases as the excess resin is drawn out of the cavity and the reinforcement is subjected to a ‘wet compaction’. Compaction behaviour of the CSM has been characterised using an Instron universal testing machine in force control mode, using a rig composed of two flat platens. Data has been fitted to a power law model;

$$V_f = V_{f0} \cdot \sigma_f^{\,B}, \tag{9}$$

where V_{f0} and B are parameters determined from experiment (see Table 1).

Currently the RI simulation only incorporates two compaction models, the dry compaction and wet compaction models giving the best fit to the experiment. However, more works needs to be done on characterisation of compaction behaviour; the loading rate and the time dependency seeming to greatly influence this behaviour.

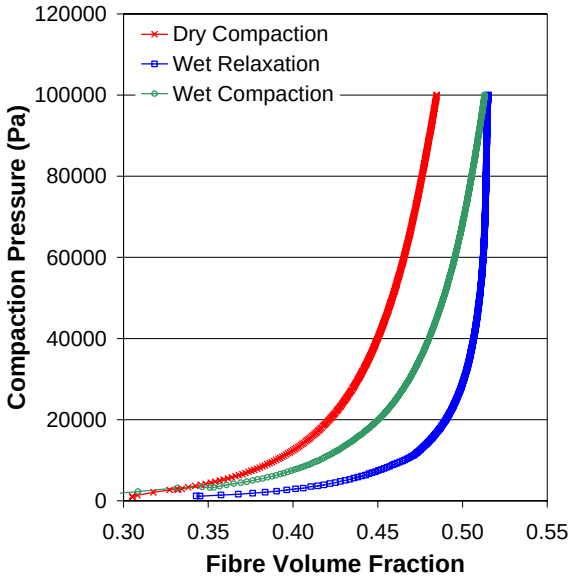

Fig. 2 Experimental compaction behaviour.

Table 1 Parameters defining the CSM compaction models

	V_{f0}	B
Dry compaction (pre-filling)	0.154	0.1007
Wet relaxation (filling)	0.253	0.0641
Wet compaction (post-filling)	0.145	0.1083

SIMULATION

Solution Method

Using the Galerkin Finite Element Method, the weak formulation of the governing equation is:

$$\int_{x_i}^{x_{i+1}} \left(\left(\frac{K}{\mu} h \frac{\partial p}{\partial x} \frac{d\omega}{dx} \right) + \frac{\partial h}{\partial t} \omega(x) \right) dx = \left[\frac{K}{\mu} h \frac{\partial P}{\partial x} \omega(x) \right]_{x_i}^{x_{i+1}}. \tag{10}$$

To assemble this formulation on the computational mesh, it is first formulated in a matrix format:

$$\overline{K\left(\bar{h}\right)_{el}} + \overline{\overline{C_{el}}}\frac{\partial \bar{h}}{\partial t} = \overline{F\left(\bar{h}\right)_{el}}, \tag{11}$$

where $\overline{K\left(\bar{h}\right)_{el}}$ is the element stiffness vector, $\overline{\overline{C_{el}}}$ is the element capacitance matrix, $\overline{F\left(\bar{h}\right)_{el}}$ is the element force vector, and $\bar{h}$ is the vector of thickness values associated with the element. An implicit method is used by applying a backward difference approximation:

$$\frac{\partial h}{\partial t} \approx \frac{h(t) - h(t - \Delta t)}{\Delta t}. \tag{12}$$

The current height values (*h(t)*) are estimated, and an iterative approach is taken to refine the solution. Eqn. 11 can then be expressed as:

$$\overline{K\left(\overline{h(t)}\right)} + \overline{\overline{C}}\left(\frac{\overline{h(t)} - \overline{h(t-\Delta t)}}{\Delta t}\right) = \overline{F\left(\overline{h(t)}\right)}, \tag{13}$$

where $\overline{h(t)}$ and $\overline{h(t-\Delta t)}$ are the vectors of height throughout the filled part of the mould at time *t* and *t-Δt* respectively. The estimated error is the residual $\overline{R\left(h(t)\right)}$, calculated from:

$$\overline{R\left(h(t)\right)} = \overline{\overline{C}}\left(\overline{h(t)} - \overline{h(t-\Delta t)}\right) + \Delta t\left(\overline{K\left(\overline{h(t)}\right)} - \overline{F\left(\overline{h(t)}\right)}\right). \tag{14}$$

To minimise the residual at each time step, the Newton-Raphson algorithm is used.

Boundary Conditions

During filling, the inlet node has a prescribed fluid pressure, and the flow front node is set to the applied vacuum pressure. During post-filling, to model clamping of the inlet tube, the inlet node is assigned a zero pressure gradient. The flow front node pressure is maintained at a constant vacuum pressure. At both inlet and vent ends of the preform, additional elements are used to simulate the distribution tape applied in these regions. This allows for more accurate simulation of the conditions at the entry and exit of the preform.

Floating Node

To allow for accurate tracking of the flow front without penalising computational performance, a floating node is used at the flow front. The mesh is composed of fixed nodes constructed at the beginning of the simulation, and one floating node is added to mark precisely the flow front. Fig. 2a describes the use of the floating node. At the start of time step *n* the laminate thickness profile is known, thus so are the V_f, permeability and fluid pressure. The flow front velocity is then approximated. The new position of the flow front is then approximated, assuming the velocity remains constant throughout the time step. The floating node is then moved to this new position and the laminate thickness profile is calculated using the Newton-Raphson implicit method.

Fig. 2b presents the convergence and performance of a simulation of the experiment presented in this paper. The fill time converges within 5 % using 60 nodes and within 1 % with 150 nodes.

With 150 elements, the run-time was 42 s using a Pentium® 4 processor with a clock speed of 3GHz and 1GB of RAM. This included the pre-filling, filling and 3000 s of post-filling.

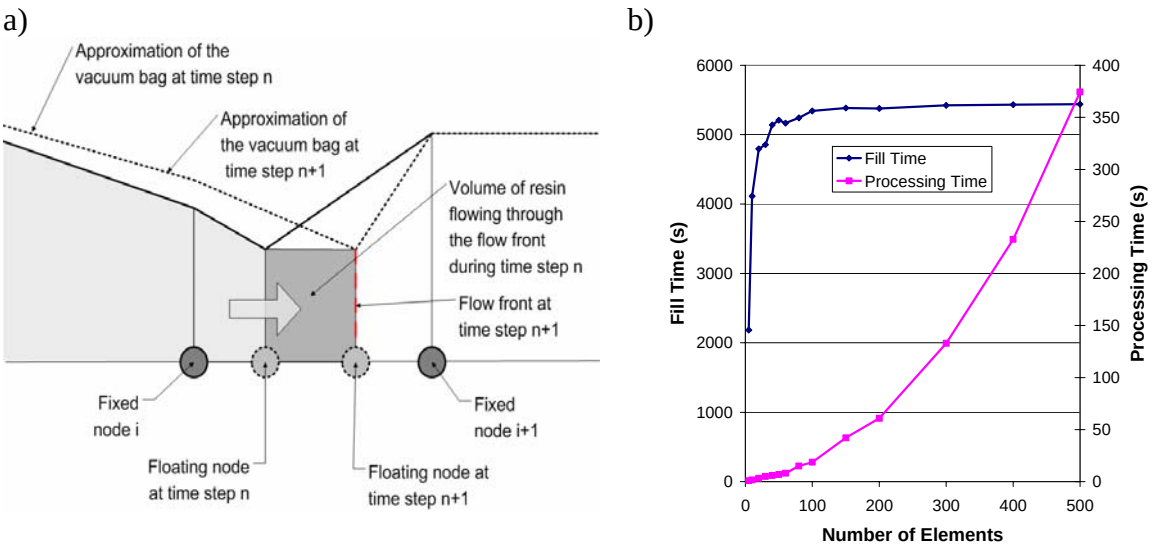

Fig. 3 a) Schematic diagram of the use of the floating node.
b) Convergence and performance plots of the simulation.

EXPERIMENTAL PROGRAM

Materials

At both inlet and vent, a 100 mm wide band of 4 mm thick flow distribution tape was laid to connect the inlet and vacuum tube to the preform. The preform was composed of ten layers of the 450 g/m^2 CSM. To avoid complications due to varying viscosity caused by the polymerisation of the resin, the RI experiment was performed using a mineral oil with Newtonian viscosity. The oil used was Mobil DTE Heavy with a viscosity of 0.182 Pa.s at 27°C.

Experimental Equipment

The setup used to monitor the RI experiment is detailed in [6]. The mould is temperature controlled and has three pressure transducers fitted to measure fluid pressure within the laminate. The resin flow rate is measured with a mass balance by monitoring the mass of the resin pot. The laminate thickness is monitored using a stereo-photogrammetry system, which records thickness variation over the entire laminate surface every 20 s. The flow front progression is tracked using the photographs taken by the stereo-photogrammetry system.

Experimental Observations

The mould temperature was maintained at 27°C during the process. In Fig. 4, the V_f has been calculated from the thickness distribution, and then averaged across the width of the mould. The surface presents the evolution over time of the V_f along the length of the laminate. During filling,

there was no apparent dip in the laminate thickness due to the lubricating effect. The V_f decreased at the inlet from 0.48 to 0.35 during filling, which was completed in 87 min. The inlet was clamped just as the fluid reached the end of the preform. After 80 min of post-filling, there is still a large gradient in the volume fraction of the preform between the inlet and the vent.

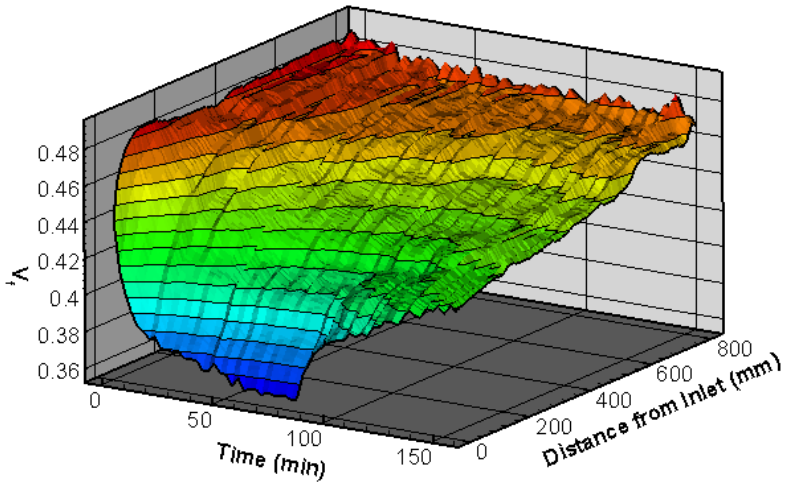

Fig. 4 Evolution over time of V_f along the length of the preform.

VALIDATION OF THE SIMULATION

Fig. 5 presents the progression of the flow front during the RI experiment, as compared to that calculated by the RI simulation. Three RTM simulation are also plotted for comparison, each utilising constant laminate thickness. For the 'Dry Case', laminate thickness is derived from the dry CSM compaction, with applied compaction equivalent to one atmosphere. The 'Wet Case' simulation uses the wet CSM compaction data at the same compaction level. The 'Inlet Case' uses the measured laminate thickness of the inlet at the end of filling. Flow front progression predicted by the RI simulation is in excellent agreement with the experimental results. The RTM 'dry' and 'wet' cases significantly over estimate the fill time, as they do not account for increases in permeability in the saturated part of the preform. The RTM 'inlet case' greatly underestimates the fill time, as an overly large cavity thickness is applied, which permeabilities significantly larger than experienced in reality.

Fig. 6 presents the comparison of the laminate thickness at three discrete points (x = 25, 350 and 775 mm) between experiment and simulation. Fig. 7 presents the experimental and simulated fluid pressure evolution at the same three points. The simulation, using purely elastic models, shows a drop in thickness just behind the flow front, due to the lubricating effect of the fluid on the fibrous reinforcement. During the experiment, this effect is not visible. This might be explained by the fact that the change in reinforcement rigidity is not instantaneous, and fluid pressure increases quickly behind the flow front, thus negating the lubricating effect. Apart from this issue, excellent agreement is attained for the thickness and pressure data.

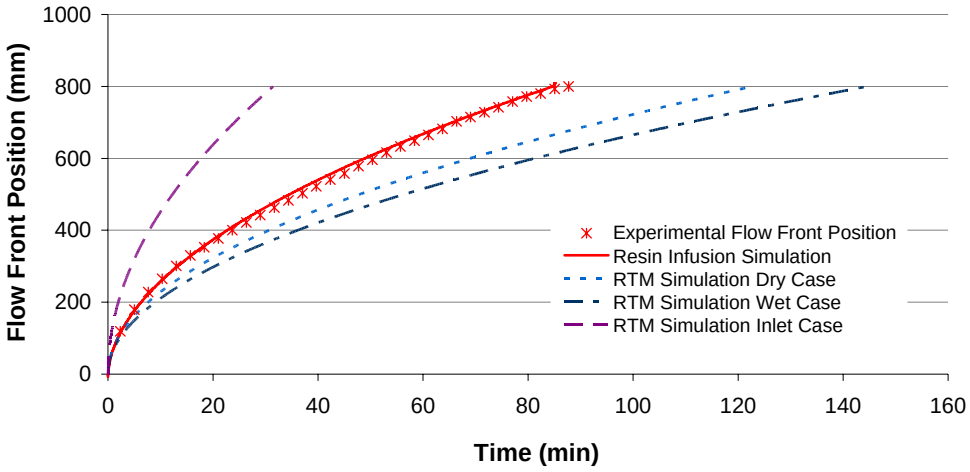

Fig. 5 Experimental and numerical evolution of flow front.

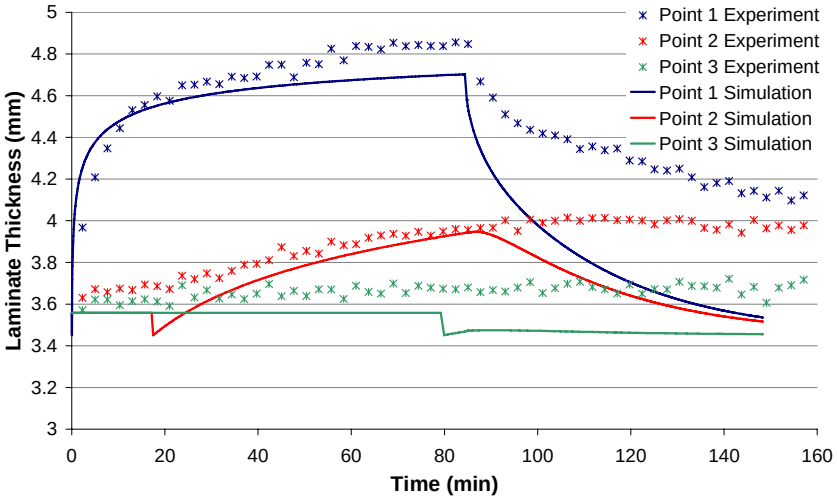

Fig. 6 Comparing experimental and simulated cavity thickness at discrete points.

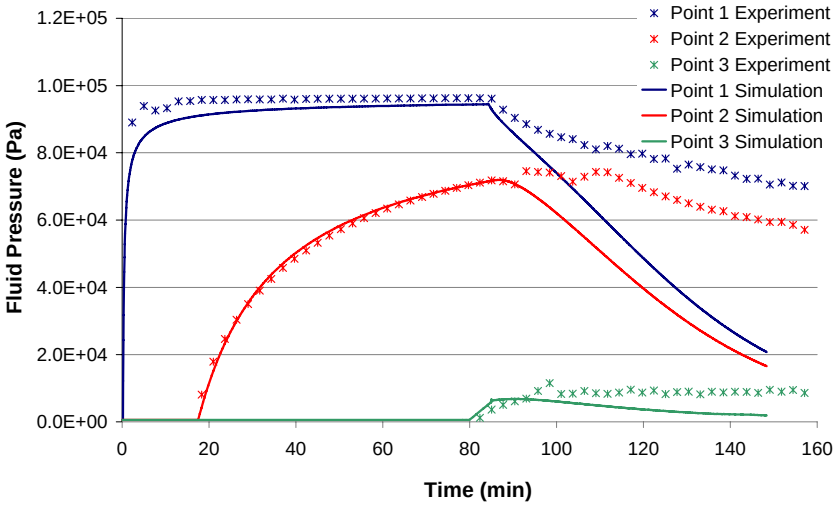

Fig. 7 Comparing experimental and simulated fluid pressure at discrete points.

During post-filling, the simulated pressure and thickness data reduce at a significantly greater rate than witnessed during the experiment. Thickness at point 2 remains essentially constant. Fluctuation in resin pressure (particularly at point 2) indicates the possibility of a vacuum leak developing at the onset of post-filling. Further experimentation is therefore required. In addition, the fluid distribution tape placed at the inlet and vent requires more careful characterisation. While the performance of the simulation during post-filling requires investigation, the results of this initial attempt to model this portion of the process are encouraging.

CONCLUSION

A one-dimensional simulation of the Resin Infusion process has been presented, addressing the pre-filling, filling and post-filling stages. Comparisons were made to a detailed experiment, using a full field laminate thickness measurement via stereophotogrammetry, as well as resin pressure monitoring. The predictions show very good agreement with the experiment during the filling stage, while the authors acknowledge that the choice of compaction model needs further research. The predictions during post-filling are promising, this simulation showing the potential for predicting V_f in the final part, as well as simulating different injection strategies (i.e. clamping of the inlet before the flow front reaches the end of the preform, or changing vacuum pressures during post-filling). Further experimentation is required to explore the quantitative mismatch during this period, including improved characterisation of materials used at the inlet and vent.

REFERENCES

1. P. A. Kelly and S. Jennings, "Nonconforming Elements for Liquid Composite Molding Processes", *Proceedings of FPCM8, Douai, France*, 2006, pp. 315.

2. F. Robitaille and R. Gauvin, "Compaction of Textile Reinforcements for Composites Manufacturing. I: Review of Experimental Results", *Polymer Composites*, Vol. 19, no. 2, 1998, pp. 198.

3. B. W. Grimsley, P. Hubert, X. Song, R. J. Cano, A. C. Loos and R. B. Pipes, "Flow and Compaction during The Vacuum Assisted Resin Transfer Molding Process", *Proceedings of International SAMPE Technical Conference*, 2001, pp. 140.

4. J. F. A. Kessels, A. S. Jonker and R. Akkerman, "Fully 2 1/2D Flow Modeling of Resin Infusion Under Flexible Tooling Using Unstructured Meshes and Wet and Dry Compaction Properties", *Composites Part A: Applied Science and Manufacturing*, Vol. 38, no. 1, 2007, pp. 51.

5. A. A. Somashekar, S. Bickerton and D. Bhattacharyya, “Exploring the Non-Elastic Compression Deformation of Dry Glass Fibre Reinforcements”, *Composites Science and Technology*, Vol. 67, no. 2, 2007, pp. 183.

6. Q. Govignon, S. Bickerton, and J. Morris, "Full Field Monitoring of Resin Flow and Laminate Properties during the Resin Infusion Moulding Process", accepted in *Composites Part A: Applied Science and Manufacturing*, 2008.